BIODIVERSITAS
Volume 25, Number 1, January 2024
Pages: 177-185

ISSN: 1412-033X
E-ISSN: 2085-4722
DOI: 10.13057/biodiv/d250120

Assessment of the dynamic growth and potassium solubilization capability of three novel bacteria

IMAM HARTONO BANGUN[1], BUNGA RAYA KETAREN[2,♥], ASRITANARNI MUNAR[1], PERDINANTA SEMBIRING[3], NURHAJIJAH[1], ANDRI ABDI[1], REYZA SUWANTO SITORUS[4]

[1]Program of Agrotechnology, Faculty of Agriculture, Universitas Muhammadiyah Sumatera Utara. Jl. Kapten Muchtar Basri 3, Medan 20238, North Sumatra, Indonesia

[2]Program of Agricultural Technology, Faculty of Agriculture, Universitas Muhammadiyah Sumatera Utara. Jl. Kapten Muchtar Basri 3, Medan 20238, North Sumatra, Indonesia. Tel.: +62-616-622400, ♥email: bungarayaketaren@umsu.ac.id

[3]Research Center for Horticulture and Estate Crops, National Research and Innovation Agency. Jl. Raya Jakarta-Bogor Km. 46, Cibinong, Bogor 16915, West Java, Indonesia

[4]Program of Agribusiness, Faculty of Agriculture, Universitas Muhammadiyah Sumatera Utara. Jl. Kapten Muchtar Basri No. 3, Medan 20238, North Sumatra, Indonesia. Tel.: +62-61-6622400

Manuscript received: 24 August 2023. Revision accepted: 21 January 2024.

Abstract. *Bangun IH, Ketaren BR, Munar A, Sembiring P, Nurhajijah, Abdi A, Sitorus RS. 2024. Assessment of the dynamic growth and potassium solubilization capability of three novel bacteria. Biodiversitas 25: 177-185.* Clay minerals are essential components that play a crucial role in soil cation exchangeable capacity and optimal plant growth. These components, including potassium (K), have the ability to bind with mineral crystals in the soil. Several studies have shown that K-solubilizing bacteria can facilitate the solubility of potassium, leading to optimal availability. However, the use of bacteria as biofertilizers is still limited due to challenges related to survival and growth patterns. To address these challenges, it is important to monitor the growth of the microbes and enhance their selection process to achieve effective utilization. Therefore, this study aimed to determine the bacterial growth dynamics and potential of *Burkholderia paludis* IHB_01, *Burkholderia cepacia* IHB_02, and *Paraburkholderia phymatum* IHB_03 in enhancing soil cation availability on clay minerals. The results showed a common initial adaptation phase among the 3 bacterial strains, followed by distinct exponential growth patterns. *Burkholderia cepacia* IHB_02 had the longest exponential growth phase, showing efficient resource utilization and extended growth. The results of soil cation enhancement by these bacteria showed that there were no major changes in measured parameters, such as total K, CEC, pH, and organic carbon. Furthermore, the variation in K exchange, organic carbon, and Na exchange provided insights into their unique interactions in the soil. The non-significant impact on potassium-related parameters in this study could be attributed to the presence of antagonistic cation interactions.

Keywords: Biofertilizer, *Burkholderia cepacia*, *Burkholderia paludis*, clay minerals, feldspar, *Paraburkholderia phymatum*, potassium

INTRODUCTION

Soil is an essential natural resource for human civilization, which supports plant growth, provides nutrients, and purifies water (Adhikari and Hartemink 2016). Furthermore, soil fertility is crucial for productive and sustainable agriculture, and it is influenced by various factors, such as mineralogy and microorganisms (Bhunia et al. 2021). Among these factors, potassium (K) has been reported to play an essential role in fertility and plant growth, and is often required in larger quantities compared to other nutrients, except nitrogen (N) (Wang et al. 2013). Despite the importance of K in the soil, a significant challenge remains its availability, particularly due to fixation in the clay mineral. Several studies have reported various factors influencing the fixation of the nutrient, including clay type and quantity, wetting-drying and freezing-thawing cycles, pH, K fertilizer application, moisture level, and the ratio of K to calcium (Ca) and magnesium (Mg) (Shakeri and Abtahi 2019). Compared to ammonium, its fixation often occurs when it binds to clay minerals and organic matter, reducing its availability for plants (Scherer et al. 2014). Clay minerals also serve as a reservoir for K, allowing for a quantitative evaluation of the nutrient (Barré et al. 2008). Previous studies have shown that K ions, which are initially considered non-exchangeable when trapped in the interlayer sites of clay minerals, can still be partly accessible and available to plants (Hinsinger et al. 1992; Falk and Krogstad 2005; Officer et al. 2006).

The limited presence of K often leads to the use of inorganic fertilizers by farmers to improve yields. However, the persistent application of these fertilizers, such as K chloride or K sulfate (K_2SO_4) in agriculture can lead to a negative K balance, showing a deficiency in acidic soils (Qaswar et al. 2020). To address this challenge, there has been widespread development in the use of environmentally friendly alternatives derived from sources, such as poultry, fisheries, and agricultural waste (Idris et al. 2023). The use of fertilizers has also been reported to have a significant effect on the soil's bacterial and fungal communities, with organic types promoting greater bacterial diversity compared to the chemical variant (He et al. 2008). The intensification of agriculture, comprising the application of high-yielding crop varieties, fertilizers, irrigation, and pesticides, contributes to soil degradation (Maranguit et al.

2017). To ensure environmental sustainability and improve the nutritional value of food, agriculture must adopt innovative methods and advanced fertilizer programs. This includes the utilization of bacteria to solubilize minerals, thereby enhancing nutrient availability and promoting optimal plant growth. A promising method to mitigate the adverse impacts of climate change on agriculture comprises the use of biofertilizers.

Recent discoveries have identified 2 novel isolates, namely *Burkholderia paludis* IHB_01, and *Paraburkholderia phymatum* IHB_03, as proficient in solubilizing K within clay minerals. Furthermore, the well-established isolate, *Burkholderia cepacia* IHB_02, has showed K solubilization capabilities (Bangun et al. 2023). *Burkholderia cepacia* is recognized for diverse mechanisms supporting plant growth, including K and phosphorus solubilization (Zhang and Kong 2014; Zhao et al. 2014; Ghosh et al. 2016), phytohormone production (Compant et al. 2008), N fixation (Marciano Marra et al. 2012), antifungal properties (Zhao et al. 2014), plant symbiosis (Tapia-García et al. 2020), and contribution to organic matter decomposition (Elshafie and Camele 2021). Previous studies also reported the ability of *P. phymatum* to form associations with the roots of leguminous plants and engage in N fixation (Vandamme et al. 2002; Moulin et al. 2014; Cai-xia et al. 2018). Based on results, limited documentation exists concerning *B. paludis*, including its capacity to synthesize enzymes, such as phosphatase, esterase, and esterase lipase, along with producing specific types of siderophore with antimicrobial properties, including pyochelin (Ong et al. 2017). Investigation is essential to prepare bacterial isolates for field application, comprising the crucial step of observing bacterial growth curves. This process requires close observation of growth trends in these isolates over time, providing insights into their behavior and potential effectiveness in real-world agriculture. This information has significantly contributed to the commercial manufacturing of various microbial products, including antibiotics, vitamins, amino acids, enzymes, yeast, vinegar, and biofertilizers (Zakaria et al. 2019; Zahri et al. 2020).

Environmental microbiologists currently face challenges centered on comprehending microbial growth in natural environments. This understanding is essential for predicting nutrient cycle rates, microbial responses to environmental disturbances, and microbial interactions and survival (Maier and Pepper 2015; Ibrahim et al. 2020). To address these challenges, further information is needed on bacterial growth, potential, and mechanisms to enhance the availability of soil cations within clay minerals. This study provides insights into the developmental of bacterial growth and their mechanisms, as well as the potential to enhance the availability of soil cations in clay minerals. Understanding the bacterial growth of these bacterial strains and their potential in K solubilization can provide information on their efficacy as plant growth-promoting agents. Therefore, this study aimed to investigate the bacterial growth dynamics and potential of *B. paludis* IHB_01, *B. cepacia* IHB_02, and *P. phymatum* IHB_03 in enhancing soil cation availability in clay minerals.

MATERIALS AND METHODS

Study site

The study was conducted in the tissue culture laboratory of the Faculty of Agriculture, Universitas Muhammadiyah Sumatera Utara, Medan, Indonesia. Furthermore, the soil specimen was collected in Besitang, Langkat, North Sumatra, Indonesia (latitude 98°14'65.21" N; longitude 4°04'86.84" E; elevation 17 meters). The study procedures were carried out from January to May 2021.

Materials

The materials used in the implementation of this study, included Aleksandrov medium (feldspar, $CaPO_4$, glucose, yeast extract, $MgSO_4 \cdot 7H_2O$, $FeCl_3$, $CaCO_3$, distilled water, NaCl), nutrient broth (NB) medium (peptone, beef extract, NaCl, yeast extract), 0.85% NaCl, KCl, isolate of KSB (K solubilizing bacteria) from a previous study (Bangun et al. 2023) on Alexandrov media (Table 3), and soil samples as materials for potency testing (Table 1). Furthermore, the equipment used was a spectrophotometer, analytical balance, digital pH meter, centrifuge, flame photometer, and rotary shaker. The procedures were divided into two stages, and the first comprised the examination of bacterial growth curves. The second stage consisted of an experimental study for potency testing in soil media.

Research implementation

The growth curve analysis of KSB was conducted to investigate the effects of factors, such as temperature, pH, and media concentration on growth according to the Monod methodology (Monod 1949). Furthermore, the process began by reproducing three KSB isolates in 250 mL liquid NB medium, followed by culture for a day at 28 ± 2°C. To establish a standard curve, Total Plate Count (TPC) method was used, as shown in Table 2. This method comprised creating serial dilutions with ratios of 1:1, 1:2, 1:4, 1:8, and 1:16. In this procedure, 4 mL of liquid NB was added to each dilution tube, except for the 1:1 tube (Figure 1).

Table 1. The initial soil characteristic for the pot experiment

Soil samples	K Total (%)	CEC (ppm)	pH	Organic carbon (%)	K-exchange (ppm)	Ca- exchange (ppm)	Mg- exchange (ppm)	Na- exchange (ppm)
A	0.08	11.42	4.72	2.44	0.13	5.73	0.64	0.04
B	0.05	11.27	4.92	1.41	0.20	2.83	0.54	0.02
Average	0.06	11.34	4.82	1.92	0.16	4.28	0.59	0.03

Note: A: depth 0-5 cm, B: depth 6-10 cm

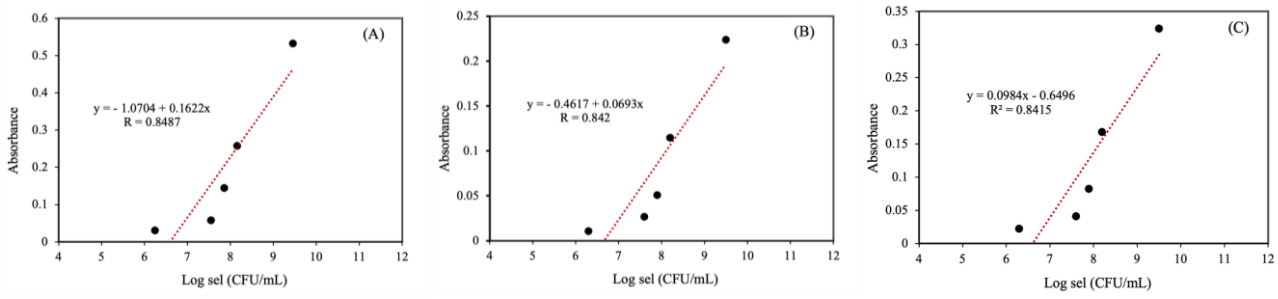

Figure 1. Standard curve of KSB based on different serial dilution conditions. A. *B. cepacia* strain IHB_02, B. *B. paludis* strain IHB_01, and C. *P. phymatum* strain IHB_03

Table 2. The standard density of KSB based on different serial dilution conditions

Serial dilutions	*B. paludis* strain IHB_01			*P. phymatum* strain IHB_03			*B. cepacia* strain IHB_02		
	Density*	Log sel*	Absorb	Density*	Log sel*	Absorb	Density*	Log sel*	Absorb
01:16	175 x 10^6	6.24	0.011	200 x 10^6	6.3	0.022	181 x 10^6	6.25	0.030
01:08	35 x 10^7	7.54	0.027	40 x 10^7	7.6	0.041	36 x 10^7	7.55	0.058
01:04	70 x 10^7	7.85	0.051	80 x 10^7	7.9	0.082	72 x 10^7	7.86	0.144
01:02	140 x 10^7	8.15	0.115	160 x 10^7	8.2	0.168	145 x 10^7	8.16	0.257
01:01	28 x 10^8	9.45	0.224	32 x 10^8	9.5	0.324	29 x 10^8	9.46	0.532

Note: *CFU mL^{-1} (CFU : colony forming unit)

Table 3. The details of the experimental treatments

Accession numbers	Bacterial isolates	Codes	Dosage KSB	Bacterial density*
-	Control (aquadest)	KSB0	10 mL pot^{-1}	-
OR342153	*Burkholderia cepacia* strain IHB_02	KSB1	10 mL pot^{-1}	34 x 10^8
OR342197	*Paraburkholderia phymatum* strain IHB_03	KSB2	10 mL pot^{-1}	35 x 10^8
OR342151	*Burkholderia paludis* strain IHB_01	KSB3	10 mL pot^{-1}	62 x 10^8

Note: *****CFU mL^{-1}(CFU = colony forming unit). Note: To ensure uniform density

The selected KSB isolates were introduced into the dilution tubes containing 8 mL of liquid NB. Subsequently, 4 mL of the solution was transferred to 1:1 tube, and 4 mL was transferred to 1:2 tube, which initially held 4 mL of liquid NB. These mixtures were thoroughly mixed, and the process was continued by transferring 4 mL of the solution from 1:2 tube to 1:4 tube and homogenized it. A total of 4 mL of the solution from the 1:4 tube was transferred to the 1:8 tube and mixed until it achieved consistent uniformity. Approximately 4 mL of the solution from the 1:8 tube was transferred to the 1:16 tube and mixed until it became homogeneous. The subsequent step comprised calibrating the spectrophotometer using liquid nutrient broth media, to adjust the measured transmittance to show a value of 100% when using this specific NB medium. Within the experiment geared towards determining the bacterial cell count using the turbidimetric method, a wavelength of 640 nm was used. A total of 1 mL of the initial culture from each of the 3 isolates was introduced into 250 mL of NB medium and placed within an incubator for 24 hours. Initial measurements were taken to ascertain the KSB cell count through a spectrophotometer set at a wavelength of 640 nm. This initial measurement established the cell concentration at the outset denoted as time t=0.

Measurements of cell density were then conducted at intervals of 30 minutes, facilitated by the spectrophotometer, extending until the culture reached a phase of stability or until a 24-hour period elapsed. The determination of cell count was accomplished by linking the logarithm of the cell count with the turbidity data derived from the 3 selected isolates, which were earlier prepared. After the calculation, the growth curve was set for analysis and assessment to determine whether noticeable alterations in growth rate occurred during the incubation period. The equation used to calculate the concentration of bacteria at a specified time is as follows Eq. 1 (Maier and Pepper 2015):

$$X = 2^n X^0 \quad \text{(Eq.1)}$$

Where:

X_0 : initial concentration of cells

X : concentration after time t

n : number of generations or cell division

In the exponential growth phase, when the initial cell count and the count at a subsequent specific time were provided, it was possible to determine the number of generations using the equation provided in Eq. 2 (Maier and Pepper 2015):

$$n = \frac{In\ X - In\ X_0}{0.693} \quad \text{(Eq. 2)}$$

Where:

n : number of generations or cell division

In : Natural logarithm (a logarithm using Euler's number (e) as the base logarithm)

X : concentration after time t

This evaluation could be performed using an appropriate equation designed for growth rate assessment Eq. 3 (Maier and Pepper 2015):

$$\mu = \frac{\mathbf{In}\ n_1 - \mathbf{In}\ n_2}{t_2 - t_1} \quad \text{(Eq. 3)}$$

Where:

μ : Growth rate

In : Natural logarithm (a logarithm using Euler's number (e) as the base logarithm)

n_2 and n_1: Number of cells at time t_2 and t_1

t_2-t_1 : Difference in time between the two measurements

The soil application experiment began by cultivating the 3 isolates in the Aleksandrov medium, followed by a 24-hour incubation period for each of them. Population quantification was achieved through TPC method with the Aleksandrov medium. Subsequently, a total of 20 pots were prepared, each containing 500 grams of sieved soil (mesh size: 40). Bacterial potency testing in soil was carried out with a non-factorial RCBD (randomized complete block design), with 5 repetitions and 4 treatment levels. A total of 500 grams of soil per pot (Table 3) was used and incubated at 28 ± 2°C for 30 days. After incubation, a comprehensive total K measurement was conducted using the HNO_3 method along with an Atomic Absorption Spectrophotometer (AAS). Further analysis, such as comprising CEC, exchangeable-K, exchangeable-Ca, exchangeable-Mg, and exchangeable-Na, were performed with the Ammonium acetate pH 7 method, while the Walkey and Black method was used to determine the organic carbon content.

Data analysis

The data obtained were subjected to statistical analysis using ANOVA. When a significant impact was detected, the subsequent examination comprised Duncan's Multiple Range Test (DMRT) at a 5% significance level. The analysis was carried out using Microsoft Excel 2016 and GraphPad Prism (Version 9.5.1) software.

RESULTS AND DISCUSSION

Growth curve of KSB2

Metabolism is a complex process comprising several anabolic (the synthesis of cell components and metabolites) and catabolic (the breakdown of cell components and metabolites) reactions. Furthermore, these biosynthetic processes led to cell division, where bacterial development could be deeply observed by monitoring the bacterial growth curve. In this study, the bacterial growth curves *B. cepacia* IHB_02, *P. phymatum* IHB_03, and *B. paludis* IHB_01 are presented in Figure 2. In a consistent and nutrient-rich culture medium, a cell could divide within 10 minutes under optimal conditions. Therefore, observations on KSB (specific term or context needed for clarity) were conducted at 30-minute intervals.

Bacterial proliferation was monitored by observing the progressive increase in the number of bacterial cells over a particular duration. Throughout the observation period, the adaptation stage of *B. cepacia* strain IHB_02 spanned from 30 to 240 minutes. Furthermore, the initial population of bacterial cells introduced through inoculation was approximately 0.0066 log cells (CFU mL^{-1}), equivalent to roughly 10 cells. The exponential phase was then observed for 240 to 960 minutes.

From the growth graph, the generation time for 8 hours was computed using Eq. 2, yielding a calculated result of n = Log 2.5890-Log 0.0066/0.693 = 4 generations. The number of generations within 8-hour timeframe was then determined as n = 4 generations. Based on this dataset, the cellular concentration (X) was determined at 8, 16, and 32 hours using Eq. 1, leading to the following: at 8 hours, X = 2^4 (10) = 16x10 cells; while at 16 hours with n = 8 generations, X = 2^8 (10) = $26x10^2$ cells; at 32 hours with n = 16 generations, X = 2^{16} (10) = $65x10^4$ cells. The specific rate of growth during the exponential phase (240-960 minutes) was determined using Eq. 3: μ = (Log 4.23-Log 0.0066)/(16 - 0) = 0.1755 cells/mL/hour.

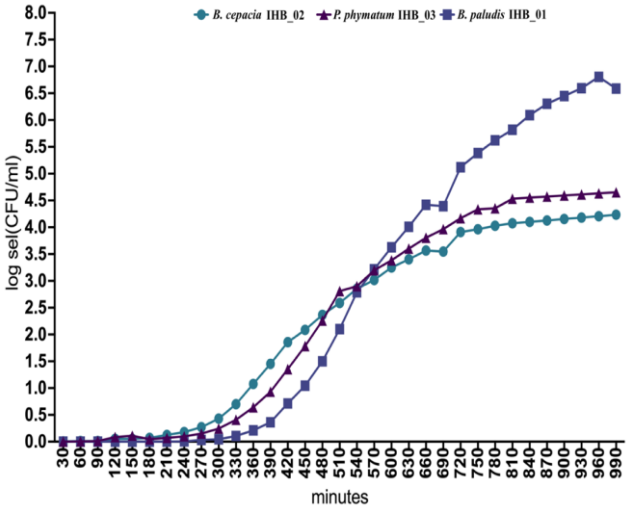

Figure 2. Growth curves of *Burkholderia cepacia* strain IHB_02, *B. paludis* strain IHB_01, and *P. phymatum* strain IHB_03 over 16 hours

Burkholderia paludis strain IHB_01 showed that the bacterial adaptation phase occurred within 30 to 330-minute timeframe. After this process, the initial population of bacterial cells introduced through inoculation was approximately 0.0066 log cells (CFU mL^{-1}), which roughly translated to 8 cells. The phase of exponential growth in these bacteria took place between 360 and 960 minutes. From the growth curve, generation time for an 8-hour duration was computed using Eq. 2, yielding a result of n = Log 2.1010-Log 0.0066/0.693 = 4 generations. Based on this dataset, the cell X was calculated at 8, 16, and 32 hours using Eq. 1 in the following manner: at 8 hours, $X = 2^4 (8) = 128$ cells; similarly, at 16 hours with n = 8 generations, $X = 2^8 (8) = 204x10^2$ cells; and at 32 hours with n = 16 generations, $X = 2^{16} (8) = 52x10^4$ cells. The specific growth rate during the exponential phase (360 - 960 minutes) was determined using Equation 3: μ = (Log 6.58-Log 0.0066)/(16-0) = 0.1875 cells/mL/hour.

For *P. phymatum* strain IHB_03, exhibited bacterial adaptation phase occurred within the time range of 30 to 270 minutes. Furthermore, the initial population of bacterial cells introduced through inoculation was approximately 0.0066 Log cells (CFU mL^{-1}), which was approximately equivalent to 10 cells. The bacterial population then entered an exponential growth phase spanning from 300 to 930 minutes. From the growth curve, the generation time for 8 hours was calculated using Eq. 2, yielded a result of n = Log 2.8084-Log 0.0066/0.693 = 4 generations. The number of generations occurring within the 8 hours was determined as n = 4 generations. Based on this data, the cell concentration (X) was calculated at 8, 16, and 32 hours using Eq. 1 as follows: at 8 hours, $X = 2^4 (10) = 160$ cells; while at 16 hours with n = 8 generations, $X = 2^8 (10) = 25x10^3$ cells; and at 32 hours with n = 16 generations, $X = 2^{16} (10) = 65x10^5$ cells. The specific growth rate during the exponential phase (300-930 minutes) was calculated using Eq. 3: μ = (Log 4.6312-Log 0.0066)/(16-0) = 0.1780 cells/mL/hour.

KSB influence on soil fertility

The results from the second phase of the experiment showed that 3 distinct KSB isolates, namely *B. cepacia* IHB_02, *P. phymatum* IHB_03, and *B. paludis* IHB_01, into the soil for 30 days yielded outcomes with no significant impact on the quantified values of total K, CEC, pH levels, and organic carbon content. These outcomes underscored the absence of significant alterations from this specific application, as shown in Figure 3

The results showed significant differences among the treatment groups regarding the total soil K content. The implementation of KSB1 led to a reduction of approximately 9.26% in the overall K levels compared to KSB0, while KSB2 and KSB3 exhibited decreases of 5.72 and 10.00%, respectively. The assessment of CEC measurements also showed notable variations. KSB1, KSB2, and KSB3 showed differences of approximately 5.85, -3.72, and +2.98%, respectively, relative to KSB0. These shifts in CEC could show alterations in the soil's ability to retain and exchangeable ion levels. The examination of pH levels showed intriguing dynamics, where KSB1 and KSB2 caused reductions of -3.47 and -5.00%, respectively. The present results suggested the engagement of a K dissolution mechanism triggered by the production of organic acids by these bacteria.

KSB3 displayed a distinctive trend, showing an increase in pH levels by 2.17% compared to KSB0. This divergence in alterations suggested varying metabolic activities among the bacterial isolates. Regarding the organic carbon observation, a similar pattern to the pH trend was observed. Organic material content decreased, with KSB1 and KSB2 contributing to reductions of -6.17% and -7.10%, respectively. The results showed that KSB3 showed a different effect, contributing to a 5.56% increase in organic carbon content compared to KSB0. These shifts in organic carbon content reflected the interplay between bacterial activities and the breakdown of organic matter. Furthermore, the illustration presented in Figure 4 provided valuable insights into the cation exchangeable process within clay minerals following a 30-day incubation period.

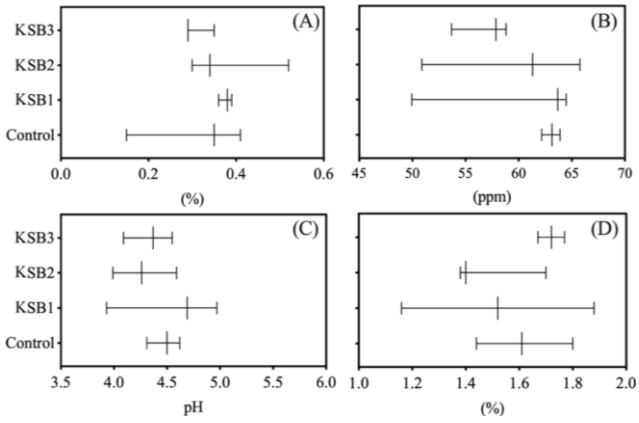

Figure 3. The effect of all KSB on the soil after 30 days of incubation on clay mineral KSB 10 ml pot^{-1} (108 CFU mL^{-1}). **(**A) K total, (B) CEC, (C) pH, and (D) organic carbon

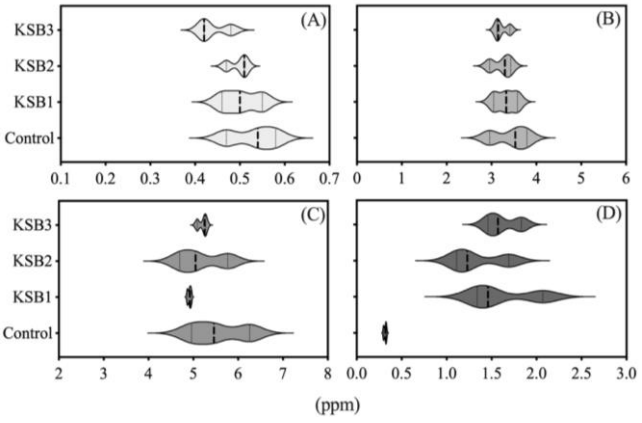

Figure 4. Cations exchangeable in clay minerals. (A) K-exchangeable, (B) Ca-exchangeable, (C) Mg-exchangeable, and (D) Na-exchangeable after 30 days of incubation

In this study, visual cues in the form of demarcations were integrated to aid in distinguishing between values on the lower and higher ends, and a central line was used to show the reference point of the mean. The data, comprising the concentrations of each cation within different treatment KSB provided intriguing insights. A closer analysis showed significant noteworthy trends and variations among the treatment groups. In observing the Na exchangeable data, it had a significant effect compared to after application to the KSB treatment. KSB1, KSB2, and KSB3 treatments showed elevated Na concentrations compared to the KSB0 group. Among these treatments, KSB2 stood out with the most significant surge in Na content, recording a concentration increase of approximately 318%. KSB3 followed closely with an increase of approximately 393%, and KSB1 exhibited a substantial increase of 406% compared to KSB0.

Based on the results, K exchangeable alterations showed no significant impact. The KSB1 treatment caused a reduction in soil K content of approximately 5.56% compared to the KSB0 group. Furthermore, both KSB2 and KSB3 showed decreases in K exchangeable, showing reductions of approximately 5.72% and 10.00% respectively. This effectively underscored and strengthened these treatments' influence on K levels. The data related to the exchangeable Ca did not show an easily identifiable pattern. Although there were slight fluctuations in Ca concentrations among the different treatment groups, these variations were not significant to definitively establish a clear impact of the treatments on the exchangeability of Ca within clay minerals. The exchangeable Mg did not show significant disparities among the treatment groups. The Mg concentrations remained relatively consistent across all treatments, without any pronounced trends or significant differences occurring after the 30-day incubation period.

Discussion

Research on bacterial growth through growth curves serves as a foundation for understanding the complex metabolic processes in bacterial cell development. Three novel discovered potassium-dissolving bacteria, namely *B. cepacia* IHB_02, *P. phymatum* IHB_03, and *B. paludis* IHB_01, were the focal points of growth analysis. Spectroscopy methods were employed to calculate bacterial growth by referring to the standard curves of each bacterium.

In the bacterial growth graph, it was observed that all three strains undergo an initial adaptation phase from around minute 30 to 240. The exponential phase of the three bacteria differs, lasting for 12 hours (minutes 240 to 960) for *B. cepacia* IHB_02, 10 hours (minutes 360 to 960) for *B. paludis* IHB_01, and 10.5 hours (minutes 300 to 930) for *P. phymatum* IHB_03. The number of generations for all three bacteria tends to be similar, occurring over 8 hours with a total of 4 generations. The concentration of cells for the three bacteria varies at each observation point (8, 16, and 32 hours). *Burkholderia cepacia* IHB_02 had a concentration of 16x10 cells at 8 hours, $26x10^2$ at 16 hours, and $65x10^4$ at 32 hours. In the case of *B. paludis* IHB_01, the cell concentration was 128 cells at 8 hours, 204 x 10^2 at 16 hours, and $52x10^4$ at 32 hours. Meanwhile, *P. phymatum* IHB_03 had concentrations of 160 cells at 8 hours, $25x10^3$ at 16 hours, and $65x10^5$ at 32 hours. The growth rate during the exponential phase was measured using the specific growth rate. During the exponential phase, the specific growth rate for *B. cepacia* IHB_02 was 0.1755 cells/mL/hours, for *B. paludis* IHB_01 it was 0.1875 cells/mL/hours, and for *P. phymatum* IHB_03 it was 0.1780 cells/mL/hours.

In the second phase, experimental results indicate that the application of KSB did not lead to substantial variations in measured parameters such as total K, CEC, pH, and organic carbon content. Although there were differences in the total soil K content, these differences were not statistically significant among the three novel bacterial strains. Additionally, differences are observed in CEC observations among treatment groups, though not statistically significant. This may indicate changes in the soil's capacity to retain and exchange ions. Based on soil pH observations, KSB3 treatment shows an increase in pH compared to the control and KSB1 and KSB2 treatments. Observations related to organic carbon content also exhibit a similar pattern to the pH trend. Data related to Na exchange show a significant impact, with all three treatments (KSB1, KSB2, KSB3) able to increase Na concentrations compared to the control. Meanwhile, data on K exchange show a different pattern, where KSB2 shows higher exchangeable K concentrations than KSB1 and KSB3. Regarding cation exchange, Ca does not show a clear pattern in all treatments and does not have sufficient significance to determine treatment effects conclusively. Meanwhile, exchangeable Mg concentrations remain fairly consistent in all treatments, without noticeable trends or significant differences after a 30-day incubation period.

Based on the results, it was clear that all three bacteria undergo an adaptation process to the new environmental conditions. This indicates that the bacteria adapt to the environmental conditions before entering the exponential growth phase. Furthermore, *B. cepacia* IHB_02 exhibits the longest exponential growth phase, followed by *P. phymatum* IHB_03 and *B. paludis* IHB_01. Bacteria *B. cepacia* IHB_02 may be more efficient in utilizing resources and experiencing a broader period of growth. The exponential growth phase emphasizes rapid bacterial division and an exponential increase in the number of cells during this phase. During the exponential phase, bacteria divide rapidly, and the number of cells increases exponentially over time (Sood et al. 2011). Disparities in cell concentrations at specific time intervals also indicate fluctuations in the length or intensity of the exponential growth phase (Schuurmans et al. 2017). It was observed that bacteria with higher concentrations may undergo a more intense exponential growth phase, a similar phenomenon also observed by Bertrand (2019), who suggesting that strains with higher concentrations may experience a longer or more intense exponential growth phase, indicating a higher ability to divide rapidly. From the data on concentrations at specific time intervals, each strain exhibits different growth rates. *Burkholderia cepacia* IHB_02 shows a lower growth rate compared to *B. paludis*

IHB_01 and *P. phymatum* IHB_03 during the observed time intervals. This variation indicates that each strain experiences a different growth rate during the exponential phase (Berney et al. 2006). This could imply differences in resource utilization efficiency and reproductive capabilities among the bacteria.

Furthermore, this study also revealed that each bacterium has its specific growth rate. The specific growth rate of *B. paludis* IHB_01 was higher compared to *B. cepacia* IHB_02 and *P. phymatum* IHB_03. Variations in specific growth rates indicate differences in genetic regulation and metabolic capacity among the bacteria (Klumpp et al. 2009). Additionally, some studies suggest that the culture environment can also influence these parameters (Ihssen and Egli 2004). These differing growth rates demonstrate the bacteria's potential for adaptation to their environment (Gonzalez and Aranda 2023). Strains with higher specific growth rate values have a better and faster ability to adapt to environmental changes (Chacón et al. 2020). Differences in temperature, nutrition, and other environmental conditions can lead to varying growth rates among the three bacteria. Understanding these parameters has implications for various applications. Strains with higher growth rates are often more valuable for industrial production or biotechnological applications. Data from growth curves, generation time, cell concentration, and specific growth rate provide insights into how bacterial metabolism and growth occur in specific culture conditions (Rolfe et al. 2012). Expanding this understanding beyond laboratory conditions is crucial for comprehending growth in natural settings or aquatic ecosystems, where challenges arise due to the complex nature of the extreme environment (Maier and Pepper 2015).

The utilization of three bacteria in the soil did not result in distinguishable variations, primarily because the K solubilization process could not occur due to the lack of supportive environmental conditions, as indicated by the total soil K content after the application of all bacteria. A key indicator in the K solubilization process, as found in some studies, involves a decrease in pH, signaling that bacteria trigger K solubilization mechanisms by producing organic acids, which is also observed in some bacteria in this study (Meena et al. 2015; Olaniyan et al. 2022). However, the differences in pH in each treatment indicate varying metabolic activities among bacterial isolates. Consistent with previous research, KSB3 can solubilize K and increase pH through mechanisms that are not yet fully understood (Bangun et al. 2023). The differences in organic carbon content in the inoculation of KSB1, KSB2, and KSB3 are attributed to disparities in the metabolic capabilities of these three strains. KSB1 and KSB2 exhibit additional activities related to the decomposition of organic matter, contributing to the decrease in organic carbon. A study suggests that bacteria belonging to the *Paraburkholderia* and *B. cepacia* groups can degrade phenolic acid compounds, thus triggering the decomposition process (Wilhelm et al. 2021). Modifications in organic carbon content reflect the complex interactions between bacterial activities and the organic matter decomposition process (Gougoulias et al. 2014; Chen et al. 2023).

The ability of all treatments to increase Na exchange can be influenced because, in general, KSB inoculation can lead to the release of K from the soil ion exchange layers, potentially increasing Na concentrations in the soil solution (Wakeel 2013). Additionally, clay soil, known for its high ion exchange capacity, may experience Na release due to KSB activity, resulting in an increase in Na concentration in the soil solution (Endo et al. 2002). The impact of KSB in clay soil affects other microbial communities and influences soil chemical conditions and ion balance, including Na. The decrease in Ca exchange after the application of KSB1, KSB2, and KSB3 may occur for several reasons. Firstly, the reduction in soil K levels due to KSB1 treatment makes K less available for ion exchange. Secondly, although KSB2 and KSB3 treatments show a decrease in K, the impact on the sufficiency of K exchange may be due to changes in how K binds to the soil structure or interacts with other ions. Thirdly, the observed decrease in K exchange after the application of KSB2 and KSB3 may also be related to the interaction between KSB bacteria and other microbes in the soil, affecting ion exchange properties. The lack of a significant influence on total K, as well as exchangeable K, Mg, and Ca, was due to antagonistic interactions among cations in the soil. According to Tan et al. (1991), antagonistic relationships between K, Ca, and Mg ions occur at soil adsorption sites due to their similar physical and chemical properties. An excess of one element can interfere with the absorption of other elements, leading to competition for soil adsorption sites. Ratios such as K/Ca, K/(Ca+Mg), and K/(Ca+Mg) provide information about soil acidity levels. Fageria (2002) suggested that despite having antagonistic properties, the ideal percentage of cation exchange saturation is 65% Ca, 10% Mg, and 5% K, or a Ca:K ratio of 13:1 and a Mg:K ratio of 2:1. This also explains the antagonism between K, Ca, and Mg. A deficiency in Mg or an excess of K can often lead to enzyme unit dissociation, halting protein formation.

In conclusion, the results of the assessment of the growth of three novel potassium-solubilizing bacteria reveal that, despite experiencing similar initial adaptation phases, *B. cepacia* IHB_02 exhibited a longer exponential growth phase, indicating efficiency in resource utilization and an extended growth period. This suggests potential added value in terms of reproduction and resource utilization. The distinct metabolic specificities among the three bacteria are reflected in their respective specific growth rates. *Burkholderia paludis* IHB_01 displays a higher specific growth rate, indicating differences in genetic regulation and metabolic capacity. The three KSB novels do not significantly impact certain parameters, such as total K, CEC, pH, and organic carbon content, but variations are observed in specific ion exchanges. *Burkholderia cepacia* IHB_02 and *P. phymatum* IHB_03 lead to a decrease in pH and organic carbon content, while *B. paludis* IHB_01 shows an increase in pH and organic carbon content. This indicates the complex role of KSB in influencing soil chemical properties. The weaknesses of

this study were that it did not observe different nutritional and environmental conditions. Therefore, further investigations should be needed on the effect of variations in nutrition, temperature, pH, and other environmental factors on bacterial growth.

ACKNOWLEDGEMENTS

The authors are grateful to the Rector of the Universitas Muhammadiyah Sumatera Utara, Medan, Indonesia for generously providing the laboratory facilities that have been instrumental in supporting the study process.

REFERENCES

Adhikari K, Hartemink AE. 2016. Linking soils to ecosystem services - A global review. Geoderma 262: 101-111. DOI: 10.1016/j.geoderma.2015.08.009.

Bangun IH, Hanum H, Sabrina T. 2023. Isolation and molecular characterization of potassium-solubilizing bacteria from limestone mountain of Bahorok, Langkat District, Indonesia. Biodiversitas 24 (7): 4175-4184. DOI: 10.13057/biodiv/d240757.

Barré P, Velde B, Fontaine C, Catel N, Abbadie L. 2008. Which 2: 1 clay minerals are involved in the soil potassium reservoir? insights from potassium addition or removal experiments on three temperate grassland soil clay assemblages. Geoderma 146 (1-2): 216-223. DOI: 10.1016/j.geoderma.2008.05.022.

Berney M, Weilenmann H-U, Ihssen J, Bassin C, Egli T. 2006. Specific growth rate determines the sensitivity of *Escherichia coli* to thermal, UVA, and solar disinfection. Appl Environ Microbiol 72 (4): 2586-2593. DOI: 10.1128/AEM.72.4.2586-2593.2006.

Bertrand RL. 2019. Lag phase is a dynamic, organized, adaptive, and evolvable period that prepares bacteria for cell division. J Bacteriol 201 (7): e00697-18. DOI: 10.1128/jb.00697-18.

Bhunia S, Bhowmik A, Mallick R, Mukherjee J. 2021. Agronomic efficiency of animal-derived organic fertilizers and their effects on biology and fertility of soil: A review. Agronomy 11 (5): 823. DOI: 10.3390/agronomy11050823.

Cai-xia L, Jing-jing Z, Ru-zhen J. 2018. Studies on the growth characteristics of nitrogen-fixing bacterium in soil of *Cunninghamia lanceolata* forest. *林业科学研究* 31 (4): 98-103.

Chacón JM, Shaw AK, Harcombe WR. 2020. Increasing growth rate slows adaptation when genotypes compete for diffusing resources. PLoS Comput Biol 16 (1): e1007585. DOI: 10.1371/journal.pcbi.1007585.

Chen W, Hu H, Heal K, Sohi S, Tigabu M, Qiu W, Zhou C. 2023. Linking microbial decomposition to dissolved organic matter composition in the revegetation of the red soil erosion area. Forests 14 (2): 270. DOI: 10.3390/f14020270.

Compant S, Nowak J, Coenye T, Clement C, Ait Barka E. 2008. Diversity and occurrence of *Burkholderia* spp. in the natural environment. FEMS Microbiol Rev 32 (4): 607-626. DOI: 10.1111/j.1574-6976.2008.00113.x.

Elshafie HS, Camele I. 2021. An overview of metabolic activity, beneficial and pathogenic aspects of *Burkholderia* Spp. Metabolites 11 (5): 321. DOI: 10.3390/metabo11050321.

Endo T, Yamamoto S, Honna T, Eneji AE. 2002. Sodium-calcium exchange selectivity as influenced by clay minerals and composition. Soil Sci 167 (2): 117-125. DOI: 10.1097/00010694-200202000-00004.

Fageria NK. 2002. Dry matter yield of common bean, lowland rice, corn, soybean, and wheat at different basic cation saturation ratios in acid soil. Commun Soil Sci Plant Anal 33 (3-4): 519-531. DOI: 10.1081/CSS-120002761.

Falk Ogaard A, Krogstad T. 2005. Release of interlayer potassium in Norwegian grassland soils. J Plant Nutr Soil Sci 168 (1): 80-88. DOI: 10.1002/jpln.200421454.

Ghosh R, Barman S, Mukherjee R, Mandal NC. 2016. Role of phosphate solubilizing *Burkholderia* spp. for successful colonization and growth promotion of *Lycopodium cernuum* L. (Lycopodiaceae) in lateritic belt of Birbhum District of West Bengal, India. Microbiol Res 183: 80-91. DOI: 10.1016/j.micres.2015.11.011.

Gonzalez JM, Aranda B. 2023. Microbial growth under limiting conditions-future perspectives. Microorganisms 11 (7): 1641. DOI: 10.3390/microorganisms11071641.

Gougoulias C, Clark JM, Shaw LJ. 2014. The role of soil microbes in the global carbon cycle: Tracking the below-ground microbial processing of plant-derived carbon for manipulating carbon dynamics in agricultural systems. J Sci Food Agric 94 (12): 2362-2371. DOI: 10.1002/jsfa.6577.

He J-Z, Zheng Y, Chen C-R, He Y-Q, Zhang L-M. 2008. Microbial composition and diversity of an upland red soil under long-term fertilization treatments as revealed by culture-dependent and culture-independent approaches. J Soils Sediments 8: 349-358. DOI: 10.1007/s11368-008-0025-1.

Hinsinger P, Jaillard B, Dufey JE. 1992. Rapid weathering of a trioctahedral mica by the roots of ryegrass. Soil Sci Soc Am J 56 (3): 977-982. DOI: 10.2136/sssaj1992.03615995005600030049x.

Ibrahim S, Abdul Khalil K, Zahri KN, Gomez-Fuentes C, Convey P, Zulkharnain A, Sabri S, Alias SA, González-Rocha G, Ahmad SA. 2020. Biosurfactant production and growth kinetics studies of the waste canola oil-degrading bacterium *Rhodococcus erythropolis* AQ5-07 from Antarctica. Molecules 25 (17): 3878. DOI: 10.3390/molecules25173878.

Idris M, Bangun IH, Ani N, Hutagaol D, Siddik F. 2023. The effect of fish waste and duck manure on the growth and yield of pak choi. J Water Land Dev 59 (X-XII):100-107. DOI: 10.24425/jwld.2023.147234.

Ihssen J, Egli T. 2004. Specific growth rate and not cell density controls the general stress response in *Escherichia coli*. Microbiology 150 (6): 1637-1648. DOI: 10.1099/mic.0.26849-0.

Klumpp S, Zhang Z, Hwa T. 2009. Growth rate-dependent global effects on gene expression in bacteria. Cell 139 (7): 1366-1375. DOI: 10.1016/j.cell.2009.12.001.

Maier RM, Pepper IL. 2015. Bacterial growth. E Environmental Microbiology (Third edition), Elsevier, Academic Press. DOI: 10.1016/B978-0-12-394626-3.00003-X.

Maranguit D, Guillaume T, Kuzyakov Y. 2017. Land-use change affects phosphorus fractions in highly weathered tropical soils. Catena 149: 385-393. DOI: 10.1016/j.catena.2016.10.010.

Marciano Marra L, Fonsêca Sousa Soares CR, de Oliveira SM, Avelar Ferreira PA, Lima Soares B, de Fráguas Carvalho R, de Lima JM, de Souza Moreira FM. 2012. Biological nitrogen fixation and phosphate solubilization by bacteria isolated from tropical soils. Plant Soil 357: 289-307. DOI: 10.1007/s11104-012-1157-z.

Meena VS, Maurya BR, Verma JP, Aeron A, Kumar A, Kim K, Bajpai VK. 2015. Potassium Solubilizing Rhizobacteria (KSR): Isolation, identification, and K-release dynamics from waste mica. Ecol Eng 81: 340-347. DOI: 10.1016/j.ecoleng.2015.04.065.

Monod J. 1949. The growth of bacterial cultures. Annu Rev Microbiol 3: 371-394. DOI: 10.1146/annurev.mi.03.100149.002103.

Moulin L, Klonowska A, Caroline B, Booth K, Vriezen JA, Melkonian R, James EK, Young JP, Bena G, Hauser L, Land M. 2014. Complete genome sequence of *Burkholderia phymatum* STM815 T, a broad host range and efficient nitrogen-fixing symbiont of *Mimosa* species. Stand Genomic Sci 9: 763-774. DOI: 10.4056/sigs.4861021.

Officer SJ, Tillman RW, Palmer AS, Whitton JS. 2006. Variability of clay mineralogy in two New Zealand steep-land topsoils under pasture. Geoderma 132 (3-4): 427-440. DOI: 10.1016/j.geoderma.2004.11.027.

Olaniyan FT, Alori ET, Adekiya AO, Ayorinde BB, Daramola FY, Osemwegie OO, Babalola OO. 2022. The use of soil microbial potassium solubilizers in potassium nutrient availability in soil and its dynamics. Ann Microbiol 72: 45. DOI: 10.1186/s13213-022-01701-8.

Ong KS, Cheow YL, Lee SM. 2017. The role of reactive oxygen species in the antimicrobial activity of pyochelin. J Adv Res 8 (4): 393-398. DOI: 10.1016/j.jare.2017.05.007.

Qaswar M, Jing H, Ahmed W, Dongchu L, Shujun L, Lu Z, Cai A, Lisheng L, Yongmei X, Jusheng G, Huimin Z. 2020. Yield sustainability, soil organic carbon sequestration and nutrients balance under long-term combined application of manure and inorganic fertilizers in acidic paddy soil. Soil Tillage Res 198: 104569. DOI: 10.1016/j.still.2019.104569.

Rolfe MD, Rice CJ, Lucchini S, Pin C, Thompson A, Cameron AD, Alston M, Stringer MF, Betts RP, Baranyi J, Peck MW. 2012. Lag phase is a distinct growth phase that prepares bacteria for exponential growth and involves transient metal accumulation. J Bacteriol 194 (3): 686-701. DOI: 10.1128/jb.06112-11.

Scherer HW, Feils E, Beuters P. 2014. Ammonium fixation and release by clay minerals as influenced by potassium. Plant Soil Environ 60 (7): 325-331. DOI: 10.17221/202/2014-PSE.

Schuurmans RM, Matthijs JCP, Hellingwerf KJ. 2017. Transition from exponential to linear photoautotrophic growth changes the physiology of *Synechocystis* sp. PCC 6803. Photosynth Res 132: 69-82. DOI: 10.1007/s11120-016-0329-8.

Shakeri S, Abtahi A. 2019. Potassium fixation capacity of some highly calcareous soils as a function of clay minerals and alternately wetting-drying. Arch Agron Soil Sci 66 (4): 445-457. DOI: 10.1080/03650340.2019.1619176.

Sood S, Singhal R, Bhat S, Kumar A. 2011. Inoculum preparation. In: Comprehensive Biotechnology (Second Edition). Academic Press. Burlington. DOI: 10.1016/B978-0-08-088504-9.00090-8.

Tan Y, Bond WJ, Rovira AD, Brisbane PG, Griffin DM. 1991. Movement through soil of a biological control agent, *Pseudomonas fluorescens*. Soil Biol Biochem 23 (9): 821-825. DOI: 10.1016/0038-0717(91)90092-X.

Tapia-García EY, Hernández-Trejo V, Guevara-Luna J, Rojas-Rojas FU, Arroyo-Herrera I, Meza-Radilla G, Vásquez-Murrieta MS, Estrada-de Los Santos P. 2020. Plant growth-promoting bacteria isolated from wild legume nodules and nodules of *Phaseolus vulgaris* L. trap plants in central and southern Mexico. Microbiol Res 239: 126522. DOI: 10.1016/j.micres.2020.126522.

Vandamme P, Goris J, Chen W-M, de Vos P, Willems A. 2002. *Burkholderia tuberum* sp. nov. and *Burkholderia phymatum* sp. nov., nodulate the roots of tropical legumes. Syst Appl Microbiol 25 (4): 507-512. DOI: 10.1078/07232020260517634.

Wakeel A. 2013. Potassium-sodium interactions in soil and plant under saline-sodic conditions. J Plant Nutr Soil Sci 176 (3): 344-354. DOI: 10.1002/jpln.201200417.

Wang M, Zheng Q, Shen Q, Guo S. 2013. The critical role of potassium in plant stress response. Intl J Mol Sci 14 (4): 7370-7390. DOI: 10.3390/ijms14047370.

Wilhelm RC, DeRito CM, Shapleigh JP, Madsen EL, Buckley DH. 2021. Phenolic acid-degrading *Paraburkholderia* prime decomposition in forest soil. ISME Commun 1 (1): 4. DOI: 10.1038/s43705-021-00009-z.

Zahri KN, Zulkharnain A, Ibrahim S, Gomez-Fuentes C, Sabri S, Calisto-Ulloa N, Ahmad SA. 2020. Kinetic analysis on the effects of lead (Pb) and silver (Ag) on waste canola oil (WCO) biodegradation by selected Antarctic microbial consortium. Malays J Biochem Mol Biol 23 (1): 20-23.

Zakaria NN, Roslee AF, Zulkharnain A, Gomez-Fuentes C, Abdulrasheed M, Sabri S, Calisto-Ulloa N, Ahmad SA. 2019. Bacterial growth and diesel biodegradation in the presence of As, Cu and Pb by Antarctic marine bacteria. Malays J Biochem Mol Biol 22 (3): 8-15.

Zhang C, Kong F. 2014. Isolation and identification of potassium-solubilizing bacteria from tobacco rhizospheric soil and their effect on tobacco plants. Appl Soil Ecol 82: 18-25. DOI: 10.1016/j.apsoil.2014.05.002.

Zhao K, Penttinen P, Zhang X, Ao X, Liu M, Yu X, Chen Q. 2014. Maize rhizosphere in Sichuan, China, hosts plant growth promoting *Burkholderia cepacia* with phosphate solubilizing and antifungal abilities. Microbiol Res 169 (1): 76-82. DOI: 10.1016/j.micres.2013.07.003.